This article was downloaded by: *[Universita di Roma La Sapienza]*
On: *1 November 2011*
Access details: *Access Details: [subscription number 939105389]*
Publisher *Taylor & Francis*
Informa Ltd Registered in England and Wales Registered Number: 1072954 Registered office: Mortimer House, 37-41 Mortimer Street, London W1T 3JH, UK

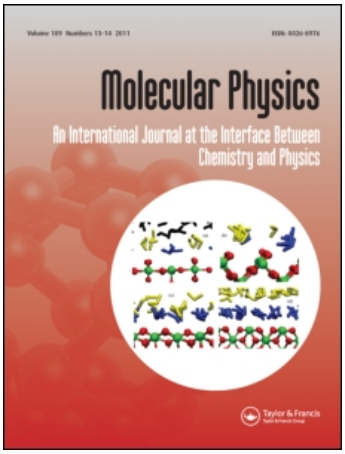

Molecular Physics
Publication details, including instructions for authors and subscription information:
http://oeh.informaworld.com/soeh/title~content=t713395160

Self and collective correlation functions in a gel of tetrahedral patchy particles

Lorenzo Rovigatti[a]; Francesco Sciortino[b]
[a] Dipartimento di Fisica, Università di Roma La Sapienza Piazzale A., 00185 Roma, Italy [b] Dipartimento di Fisica and CNR-ISC, Università di Roma La Sapienza Piazzale A., 00185 Roma, Italy

First published on: 15 September 2011

To cite this Article Rovigatti, Lorenzo and Sciortino, Francesco(2011) 'Self and collective correlation functions in a gel of tetrahedral patchy particles', Molecular Physics,, First published on: 15 September 2011 (iFirst)
To link to this Article: DOI: 10.1080/00268976.2011.609148
URL: http://dx.doi.org/10.1080/00268976.2011.609148

PLEASE SCROLL DOWN FOR ARTICLE

The American Conference of Governmental Industrial Hygienists (http://www.acgih.org/) and the American Industrial Hygiene Association (http://www.aiha.org/) have licensed the Taylor & Francis Group to publish this article and other materials. To join the American Conference of Governmental Industrial Hygienists visit http://www.acgih.org/Members/. To join the American Industrial Hygiene Association visit http://www.aiha.org/Content/BecomeMember/becomemember-splash.htm.

Full terms and conditions of use: http://oeh.informaworld.com/terms-and-conditions-of-access.pdf

This article maybe used for research, teaching and private study purposes. Any substantial or systematic reproduction, re-distribution, re-selling, loan or sub-licensing, systematic supply or distribution in any form to anyone is expressly forbidden.

The publisher does not give any warranty express or implied or make any representation that the contents will be complete or accurate or up to date. The accuracy of any instructions, formulae and drug doses should be independently verified with primary sources. The publisher shall not be liable for any loss, actions, claims, proceedings, demand or costs or damages whatsoever or howsoever caused arising directly or indirectly in connection with or arising out of the use of this material.

Molecular Physics
2011, 1–8, iFirst

Taylor & Francis
Taylor & Francis Group

SPECIAL ISSUE IN HONOUR OF LUCIANO REATTO

Self and collective correlation functions in a gel of tetrahedral patchy particles

Lorenzo Rovigatti[a]* and Francesco Sciortino[b]

[a]*Dipartimento di Fisica, Università di Roma La Sapienza Piazzale A., Moro 5, 00185 Roma, Italy;*
[b]*Dipartimento di Fisica and CNR–ISC, Università di Roma La Sapienza Piazzale A., Moro 5, 00185 Roma, Italy*

(*Received 5 July 2011; final version received 20 July 2011*)

We discuss the results of intensive Brownian dynamics simulations of a simple model of tetrahedral patchy particles in the optimal network density region. This choice allows us to investigate the evolution of the structure and of the dynamics in a wide range of temperatures without encountering any phase separation. The slowing down of the dynamics in this model system is driven by the progressive bond formation and the increasing bond lifetime. Although dynamical arrest is different from the glass case, where excluded volume interactions are dominant, the decay of the self- and collective correlation functions of the resulting fluid bears similarities with that observed in glassy systems.

Keywords: statistical physics; colloids; simulations

Downloaded By: [Universita di Roma La Sapienza] At: 16:26 1 November 2011

1. Introduction

Patchy colloidal particles [1–3] continue to be the subject of intense investigation, both experimentally and theoretically. There is indeed much expectation in the outcome of recent efforts of creating colloidal particles that interact via anisotropic potentials. The challenge faced by physicists, chemical engineers and material scientists is to organize these new geometries into specific structures via self-assembly, the spontaneous organization of matter into desired arrangements. The aim is to achieve – via the rational design of elementary building blocks (i.e. the particles) – predefined specific structures, ordered or disordered, shifting from the top-down to the bottom-up approach, in which effort is made in the direction of controlling particle shape and patterning.

Theoretical and numerical studies of the phase behavior of patchy colloidal particles have been very rewarding. Quite unexpectedly, a very rich framework for interpreting phenomena like thermoreversible gelation, the competition between gelation and glass transition or the competition between condensation and polymerization [4] has been unraveled. New concepts like empty liquids [5–7], equilibrium gels [8,9], and unconventional gas–liquid phase diagrams [10–12] have been introduced and have been very fruitful in promoting further developments [13,14]. One of the unexpected connections concerns the analogy between gelation in patchy colloids and glass formation in atomic and molecular network-forming systems [13]. Indeed, studying the role of the 'valence' M (defined here as the maximum number of possible bonded nearest neighbors) it has been disclosed that the packing fraction ϕ of the liquid coexisting with the gas decreases on decreasing M [5]. For the case of hard-sphere colloids with four patches, ϕ is of the order of 30%. This implies that, for larger values of ϕ, gas–liquid phase separation is not encountered on cooling. On progressively decreasing the temperature T, the average lifetime of a patch–patch bond increases and particles become arrested by being part of a long-lived network of bonds. Energetic bonds thus determine the slowing down of the dynamics and the approach to a non-ergodic state, a dynamical arrest that we call gelation [6,8,15,16]. Dynamical arrest can thus be expected to be different from that characterizing glassy states, where caging is controlled by excluded volume interactions. Limited valence is crucial for gelation, since only when valence is limited, is this region of intermediate densities, where packing does not play a major role, is accessible at low T. For spherically interacting colloids, the gas–liquid phase separation is much wider and the coexisting liquid density is found at $\phi \approx 0.6$–0.7. Hence, if crystallization is preempted, a liquid of spherically interacting particles can be brought to low T to form a glass without phase separating only at very large densities.

In this article we investigate in detail the evolution on cooling of the self- and collective dynamics of a model for tetrahedral patchy colloids in the gel region

*Corresponding author. Email: lorenzo.rovigatti@uniroma1.it

ISSN 0026–8976 print/ISSN 1362–3028 online
© 2011 Taylor & Francis
DOI: 10.1080/00268976.2011.609148
http://www.informaworld.com

at a fixed value of the density, in the so-called optimal network density region. In this window of densities the system is expected to be able to form an ideal (fully connected) random tetrahedral network [17]. At lower densities, gas–liquid phase separation takes place, while at larger densities packing prevents the possibility of geometrically arranging all molecules with the proper angular and distance constraints required to form bonds. Despite the different nature of the dynamical arrest process, driven by bonding rather than by packing, the decay of the correlation functions for this four-coordinated model resembles that observed in glasses.

2. Model and numerical methods

We study a simple continuous model for tetrahedral patchy particles by means of Brownian dynamics simulations. A particle is modeled as a rigid body defined by the position of its center of mass and by $M = 4$ vectors indicating the locations of the four patches [6]. The interaction potential between particles 1 and 2 is

$$V(1,2) = V_{CM}(1,2) + V_P(1,2) \tag{1}$$

where V_{CM} is the potential acting between the centers of mass of the two particles and V_P is the interaction between patches:

$$V_{CM}(1,2) = \left(\frac{1}{r_{12}}\right)^m \tag{2}$$

$$V_P(1,2) = -\sum_{i=1}^{M}\sum_{j=1}^{M} \epsilon \exp\left[-\frac{1}{2}\left(\frac{r_{12}^{ij}}{\alpha}\right)^n\right]. \tag{3}$$

The large value $m = 200$ is chosen to approximate the hard-sphere behavior, the quantity $n = 10$ makes the exponential function resemble a square well, $\alpha = 0.12$ guaranties that the single bond per patch condition is satisfied and $\epsilon = 1.001$ fixes the absolute minimum at unitary depth. The distance between the centers of particles 1 and 2 is indicated as r_{12} while the distance between patches on different particles is denoted by the symbol r_{12}^{ij}. Bond forces thus act on surface spots allowing momenta which can induce particle rotations.

The parameters entering in the functional form (Equations 2 and 3) have been chosen in such a way that the resulting potential has a depth $u_0 = -1$ and it resembles that resulting from respectively a hard sphere and a square well potential, allowing greater flexibility in the study of the dynamics of these systems compared to step-wise potentials. Note that, while in the Kern–Frenkel potential [18] the interaction range and the angular width of the bond can be independently controlled, in the present continuous potential the patch–patch interaction depends only on the patch–patch distance and hence the patch–patch interaction range and angular width are coupled.

We perform Brownian dynamics simulations in the NVT ensemble using 10,000 particles in a cubic box of size $L = 26$ with periodic boundary conditions. In the following, the energy unit is chosen to be the depth u_0 of the potential, the length unit is chosen to be the colloid diameter σ and time is in units of $\sigma\sqrt{m/u_0}$, where m is the mass of the colloids. The Brownian algorithm used in the simulations is described in the appendix of Ref. [6]. Here we summarize its features. A Velocity Verlet integrator with a time-step $\delta t = 0.001$ is used to integrate the equations of motion. To model Brownian diffusion, we define a probability p for each particle to undergo a random collision every $\mathcal{N}$ time-steps. By tuning p it is possible to obtain the desired free particle diffusion coefficient D_0 using the relation

$$D_0 = \frac{k_B T \mathcal{N} \delta t}{m}\left(\frac{1}{p} - \frac{1}{2}\right). \tag{4}$$

In simulation units the chosen translational bare diffusion coefficient is $D_0^T = 0.01$ and the corresponding rotational diffusion coefficient is $D_0^R = 0.03$ (so that $D_0^R/D_0^T = 3$, as expected for non-slip particles). These values fix p^T and p^R for each temperature.

The average time between two random collisions is given by

$$\Delta t = \frac{\mathcal{N}\delta t}{p} = \frac{k_B T \mathcal{N} \delta t + 2mD_0}{2k_B T}, \tag{5}$$

thus our simulations follow Newtonian dynamics for $t < \Delta t$ and Brownian dynamics after that time.

In order to equilibrate at the lowest temperatures we implemented a version of the code that runs on GPUs using CUDA [19]. The simulations were performed on Tesla C2050 GPUs. While on this hardware peak performances can be achieved only if single precision is used, the numerical instability makes it unfeasible to use float precision [20]. To overcome these instabilities but still retain good performances we use double precision for time integration and single precision for force calculation [20,21]. While using full double precision results in a two-fold performance loss, using this mixed single-double precision results only in a 10–15% decrease in performance.

The performances achieved on GPUs depend heavily on interaction details (such as cut-off distances), number of particles and density [20–23]. For the state points investigated in this work

Downloaded By: [Universita di Roma La Sapienza] At: 16:26 1 November 2011

Downloaded By: [Universita di Roma La Sapienza] At: 16:26 1 November 2011

($N = 10{,}000$, $\rho\sigma^3 = 0.57$) we obtained a 30× speed-up with respect to a Xeon E5620 (single core).

We have used up to 10^{10} MD steps for equilibration and from 10^7 to $2 \cdot 10^9$ MD steps for data generation, depending on the temperature.

In Brownian dynamics simulations particles are subject to a random force which accounts for the collisions between colloidal particles and the solvent. Even if the random force has a zero mean, the position of the center of mass of the system becomes a random variable, again with zero mean. In standard simulations the random motion of the center of mass (COM) is negligible and the particle dynamics is weakly affected by this random process. In the study of very long simulations, such as those reported here (which extend to more than 10^9 integration time-steps), the motion of the center of mass can be quite substantial and can produce artifacts in the evaluation of dynamical quantities. For this reason, in all data presented in this work the trajectories of the single particles have been corrected to subtract the center of mass motion. Care needs to be taken in the analysis of Brownian dynamics trajectories in glassy systems, especially now that the increased power of GPUs for scientific application is opening the possibility of investigating arrested states via lengthy simulations.

3. Results

3.1. *Static properties*

To properly frame the investigation of the dynamics, we start by showing in Figure 1(a) the potential energy per particle as a function of T. The energy has the typical sigmoidal shape characteristic of bond interactions, reminiscent of the two-state behavior of the bonds (broken or formed). On cooling, the system changes from a collection of isolated clusters to a percolating network to an essentially fully bonded configuration, with a few isolated monomers detaching from the infinite cluster, as indicated by the cluster size distribution, reported in Figure 1(b). Two particles are considered connected, and hence belonging to the same cluster, if their pair interaction energy is lower than -0.5. Below $T = 0.15$, a large fraction of particles belongs to the infinite cluster and at the lowest investigated T more than 99% of the particles is in the infinite cluster (see inset of Figure 1b). Hence, at low T the system can be visualized as a percolating network which incorporates most of the particles.

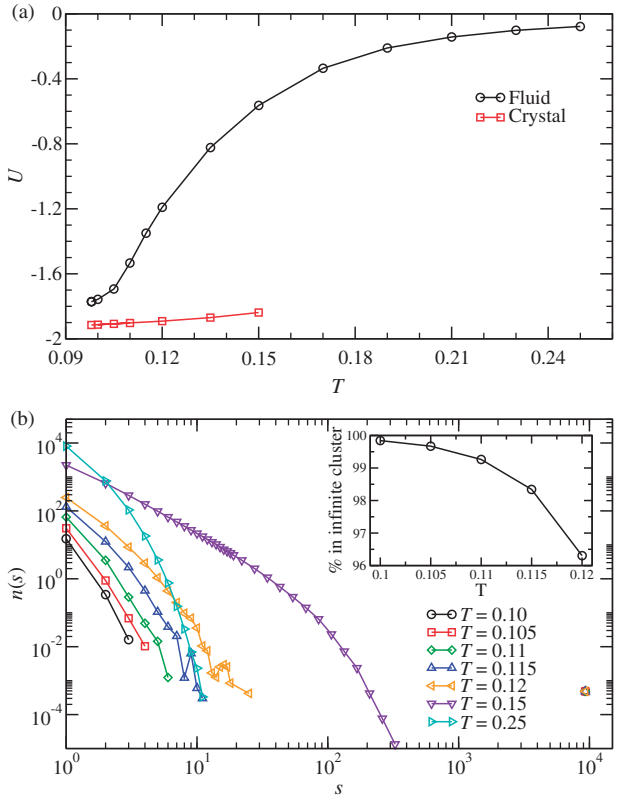

Figure 1. (a) Potential energy per particle U as a function of temperature (black circles). Also shown for comparison is the potential energy per particle in a diamond crystal structure (red squares). (b) Number of clusters $n(s)$ of size s for different temperatures for a system of 10,000 monomers. For $T < 0.15$ the system always contains a percolating cluster (disconnected points at $s \approx 10^4$). Inset: percentage of particles that are in the infinite cluster (P_∞) as a function of T. (Colour online).

3.2. *Bond Lifetime*

The bond–bond autocorrelation function $C_b(t)$, defined as the probability that a bond existing at $t = 0$ exists also at time t, provides a quantification of the typical microscopic time, setting the scale for the dynamics, separating the (short) time scale in which the dynamics takes place at fixed bonding pattern from the (long) time scale where the dynamics is intrinsically connected to bond breaking events. Figure 2(a) shows $C_b(t)$ for all the investigated T, showing that more than five orders of magnitude in bond lifetime are properly explored. The decay of the correlation function can be fitted with a stretched exponential function, $e^{-(t/\tau_b)^{\beta_b}}$, suggesting that the different local bonding environments have a role in the process of bond breaking. From the fit, an average bond time can be calculated as $\langle \tau_b \rangle = \frac{\tau_b}{\beta_b} \Gamma(\frac{1}{\beta_b})$, where $\Gamma(x)$ is the Gamma function. The values of β_b are reported in the inset of Figure 2(a), while the T dependence of τ_b and $\langle \tau_b \rangle$ is shown in Figure 2(b).

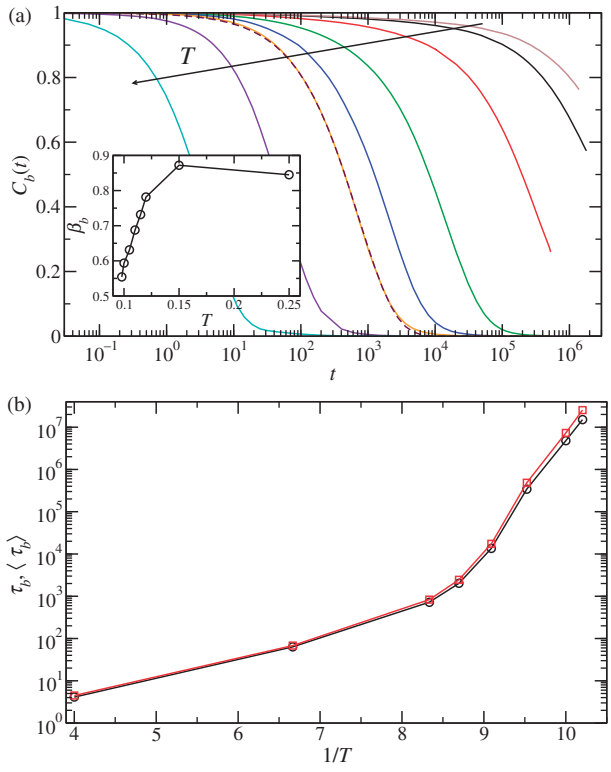

Figure 2. (a) Bond–bond autocorrelation function for different temperatures ($T = 0.098$, 0.10, 0.105, 0.11, 0.115, 0.12, 0.15, 0.25). A stretched exponential fit to $C_b(t)$ at $T = 0.12$ is also included (dashed line). Inset: values of the fit parameter β_b (see text) for different temperatures. (b) Values of the fit parameter τ_b (black circles) and the average bond time $\langle \tau_b \rangle$ (red squares, see text) for different temperatures. (Colour online).

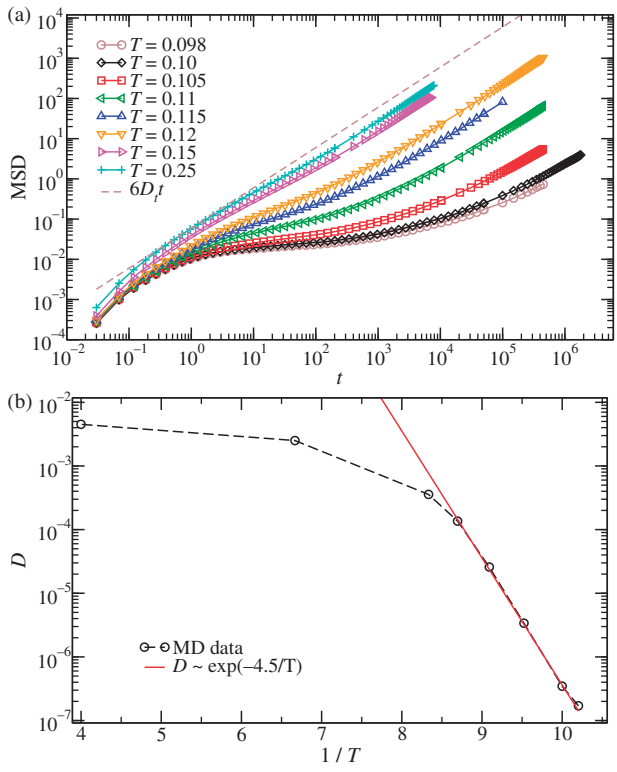

Figure 3. (a) Mean square displacement for different temperatures. The dashed line shows the expected time dependence of the diffusive behavior at long times for monomers (for which $D_t = 0.01$). (b) Diffusion coefficient D extracted from the slope of the MSD at long time for different temperatures (black circles). The red line is an Arrhenius fit performed over the five lowest temperatures. (Colour online).

3.3. *MSD and the diffusion coefficient*

Figure 3(a) shows the mean square displacement (MSD) for all the investigated T. Above and around percolation, no plateau in the time dependence of the MSD is observed. Indeed, close to $T = 0.15$, the lifetime of the bonds is still very short and no dynamical signatures of the presence of a transient infinite cluster are observed. Below percolation an inflection develops, giving rise to a plateau which increases on further cooling. The height of the inflection point significantly changes with T, signaling that bonding progressively reduces the cage volume. At the lowest T, the MSD becomes comparable to the square of the bonding distance, suggesting that in a (almost) fully bonded locally tetrahedral structure, bond confinement can be quite effective.

The diffusion coefficient D, evaluated from the long time limit of the mean square displacement ($\mathrm{MSD} = 6\ Dt$) is shown in Figure 3(b). D is clearly super-Arrhenius around the percolation temperature. In this T-interval indeed the structure of the system changes significantly, since particles first aggregate into larger and larger clusters and, beyond percolation, join more and more the spanning cluster. As discussed later on, upon entering well inside percolation the structure of the system reaches its equilibrium gel state and no further significant structural changes take place. At these low T, D shows an apparent Arrhenius behavior, with an activation energy of about -4.5, a value slightly larger than the energy required to completely break four bonds. The Arrhenius dependence classifies the present model in the category of strong glass-forming systems [24], which includes all tetrahedral network fluids. In this respect, the present results confirm once more that there is a strong connection between the insurgence of an open local structure held together by strong directional forces and the observation of Arrhenius dynamics. It is also interesting to observe that a similar value has been recently reported in the study of ST2 water at the optimal network density [25]. Values of the activation energy of the

Downloaded By: [Universita di Roma La Sapienza] At: 16:26 1 November 2011

order of four bonds have also been observed in a model of tetrahedral DNA constructs [26] and in a primitive model for water [17], suggesting that the mechanism for microscopic dynamics in tetrahedral networks shares common features.

3.4. *Self-dynamics*

To analyze the tagged particle motion in the wavevector $\vec{q}$ space, we evaluate the self-intermediate scattering functions $F_s(q,t)$, defined as

$$F_s(\vec{q},t) = \frac{1}{N}\sum_{i=1}^{N}\langle e^{-i\vec{q}\cdot(\vec{r}_i(t)-\vec{r}_i(0))}\rangle \tag{6}$$

where $\vec{r}_i(t)$ is the position of the center of particle i at time t and $q = |\vec{q}|$. The behavior of the correlation functions is shown in Figure 4 as a function of T for two different wavevector values (panels (a) and (b)) and as a function of q at $T = 0.10$ (panel (c)). To help comparing the characteristic time scales, the bond autocorrelation function is also reported. The long time decay of these functions can be rather well modeled via stretched exponentials,

$$F_s(q,t) = f_q^s e^{-(t/\tau_s(q))^{\beta_q^s}} \tag{7}$$

where f_q^s plays the role of the non-ergodicity factor, $\tau_s(q)$ is the characteristic decay time and β_q^s is the stretching exponent. The wavevector dependence of f_q^s, $\tau_s(q)$ and β_q^s is reported in Figure 5. The non-ergodicity parameter shows the typical Gaussian shape, but with an amplitude that is clearly T dependent, confirming that the cage volume decreases on cooling. A similar effect is also observed in glasses, but only below the so-called mode-coupling critical temperature [27], suggesting that somehow network liquids remain sufficiently fluid to be observed well below the point where dynamics crosses from power-law to Arrhenius. The stretching exponent is also T dependent and varies significantly on varying q. At small q, where dynamics has to convert to diffusive dynamics, β_q^s approaches one and $\tau_s(q) \sim q^{-2}$. Finally, Figure 5(c) shows $\tau_s(q)$ and Figure 5(d) shows $\tau_s(q)q^2$. It also shows the corresponding lifetime of the bond. Interestingly, the crossing between τ_b and $\tau_s(q)$ takes place to larger and larger q values on cooling, suggesting that the dynamics on smaller and smaller time scales becomes more and more slaved to the bond breaking process. Only when time has become longer than the bond-breaking time particles are able to restructure themselves and relax the density fluctuations. Figure 5(d) also shows that at the lowest investigated T, the approach to the diffusive limit is not clearly reached within the wavevector range which can be explored by our simulation.

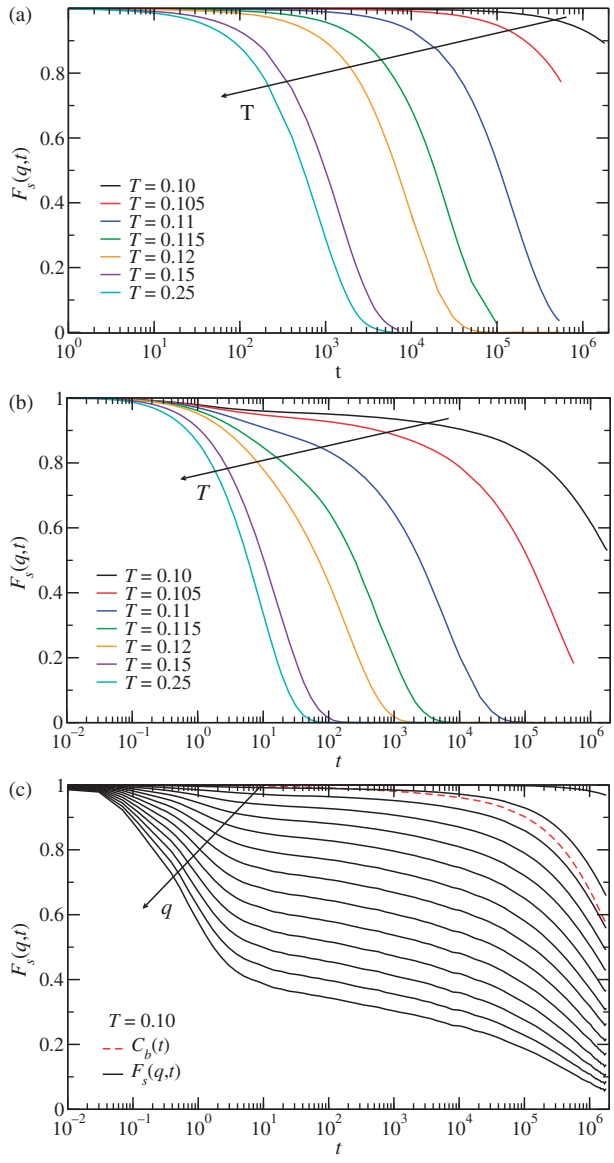

Figure 4. (a) $F_s(q,t)$ at different temperatures for $q\sigma = 0.48$. (b) $F_s(q,t)$ at different temperatures for $q\sigma = 4.59$ (corresponding to the first peak in the $S(q)$, see Figure 5e). (c) $F_s(q,t)$ at $T = 0.10$ for different values of the wavevector $q\sigma$ (0.24, 2.1, 3.9, 5.7, 7.5, 9.3, 11, 13, 15, 17, 18, 20, 22, 24). Also shown is the $C_b(t)$ at the same temperature (dashed red line).

3.5. *Collective dynamics*

To analyze the collective particle motion in wavevector $\vec{q}$ space, we evaluate the coherent intermediate scattering functions $F_c(q,t)$, defined as

$$F_c(\vec{q},t) = \frac{1}{N}\left\langle \sum_{i,j=1}^{N} e^{-i\vec{q}\cdot(\vec{r}_i(t)-\vec{r}_j(0))}\right\rangle. \tag{8}$$

As for the self-case, we show in Figure 6 the q and T dependence of the collective correlation function.

Downloaded By: [Universita di Roma La Sapienza] At: 16:26 1 November 2011

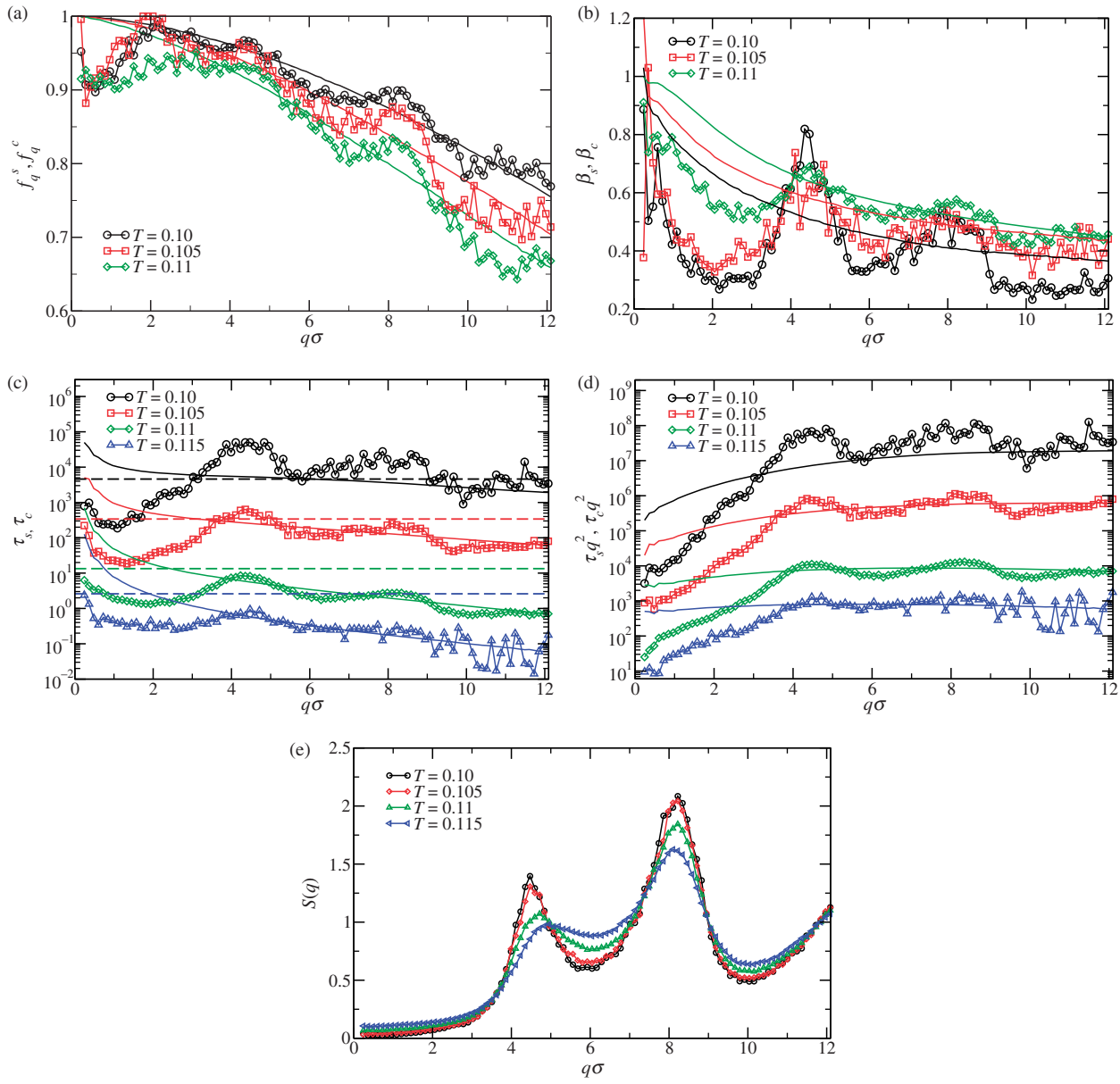

Figure 5. Fit results for the self (solid lines) and collective (symbols) intermediate scattering functions for different temperatures as functions of the wavevector. (a) Non-ergodicity factors. (b) Stretched exponents. (c) Characteristic decay times (dashed lines are τ_b, added for comparison). (d) Characteristic decay times multiplied q^2. (e) Structure factors for the lowest temperatures. (Colour online).

The data are significantly more noisy, reflecting the absence of the average over the distinct tagged particles. Despite the noise, some trends are clear and worth discussing. At low temperatures, very long times and small wavevectors, $F_c(q, t)$ shows an oscillatory behavior which has been tentatively attributed to the presence of acoustic sound modes [8]. If we use Equation (7) to fit these curves, we can note that also the collective non-ergodicity parameter shows a clear T dependence at low T. The values of f_q^c oscillate around the self ones, in phase with the position of the peaks of the structure factor $S(q)$ (see Figure 5e), similarly to what has been observed for glasses [28–30]. Beside the main peak at $q\sigma \approx 8$, the structure factor shows a pre-peak characteristic of tetrahedral networks, where the slowest collective modes are found. In passing, we note that the T dependence of $S(q)$ tends to saturate at low T ($S(q)$ at $T = 0.10$ and $T = 0.105$ are identical within the noise) suggesting that the system structure does not significantly evolve any longer with T. This saturation

Downloaded By: [Universita di Roma La Sapienza] At: 16:26 1 November 2011

Downloaded By: [Universita di Roma La Sapienza] At: 16:26 1 November 2011

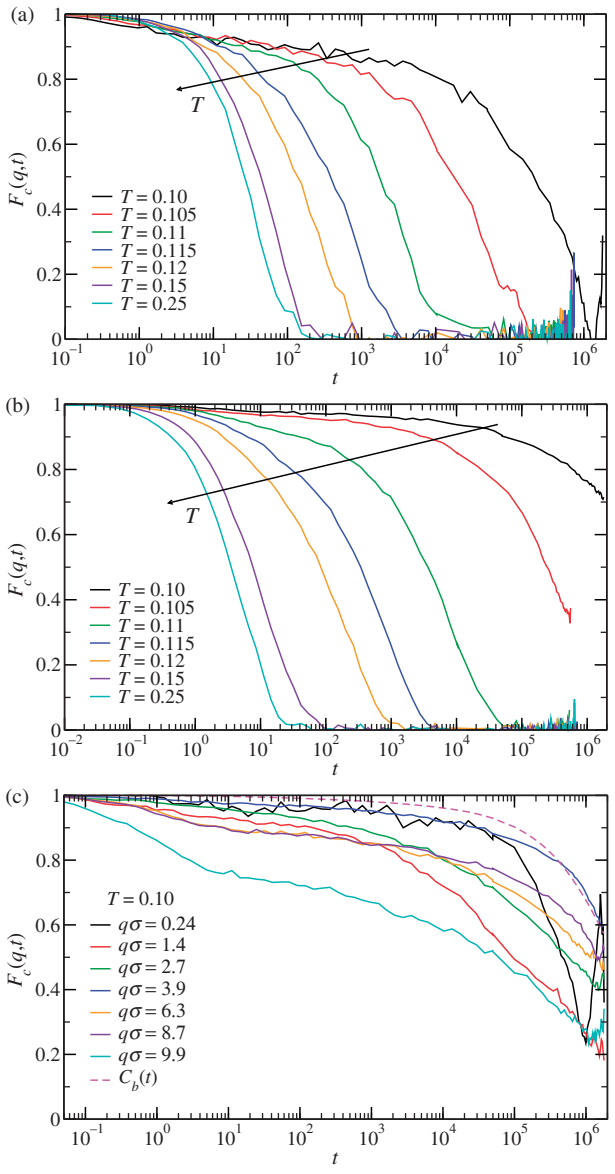

Figure 6. (a) $F_c(q,t)$ at different temperatures for $q\sigma = 0.48$. (b) $F_c(q,t)$ at different temperatures for $q\sigma = 4.59$. (c) $F_c(q,t)$ at $T = 0.10$ for different values of the wavevector. Also shown is the $C_b(t)$ at the same temperature (dashed magenta line). (Colour online).

of $S(q)$ at small T has been interpreted as evidence of an equilibrium gel state [5,31].

Interestingly, the decay of the density fluctuations does not always require the breaking of bonds. For example, at $T = 0.115$, $\tau_c(q)$ is always smaller than τ_b, suggesting that the decay of the density fluctuations at small q happens at a fixed network structure. On further cooling, $\tau_c(q)$ and τ_b get closer, and at $T = 0.10$ $\tau_c(q) \gtrsim \tau_b$ for intermediate and large values of q. This means that the breathing modes of the network,

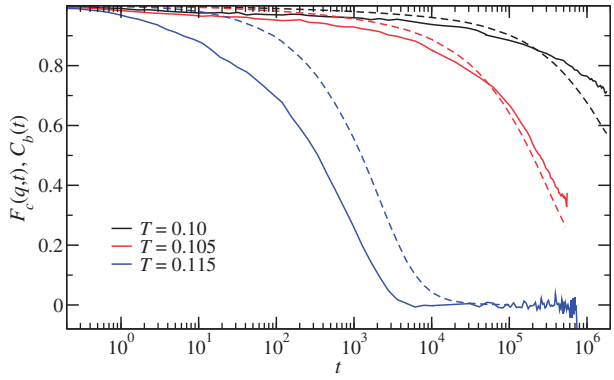

Figure 7. $F_c(q,t)$ for $q\sigma = 4.59$ (solid lines) and $C_b(t)$ (dashed lines) at three different temperatures. (Colour online).

diffusive in nature, are of sufficient amplitude to relax the density fluctuations at large wavelength. Only at very low T does the gel becomes so stiff that the decay of the density fluctuations takes place on a time scale comparable to or longer than τ_b. This is more clearly shown in Figure 7: at $T = 0.115$ the bond–bond autocorrelation decays faster than the density fluctuations at $q\sigma = 4.59$; at $T = 0.105$ the two times are similar while at $T = 0.10$ the opposite behavior is observed and the decay of the density fluctuations requires the breaking of the network to take place.

4. Conclusions

We have reported a study of the self- and collective dynamics of a simple tetrahedral patchy model for colloidal particles decorated by four attractive sites, located on the vertex of a tetrahedron. The shape and range of the site–site interaction is chosen in such a way that particles can form at most one bond per site. On cooling, the system progresses from a collection of isolated clusters to an essentially fully bonded tetrahedral network, in which most of the particles are engaged in four bonds. We have investigated the model at fixed density, in the optimal network density region. Indeed, the presence of a limited number of strong directional interactions determines a limited range of densities which are compatible with the possibility of satisfying all possible interacting sites. This optimal density region is limited at low density by the presence of gas–liquid coexistence and at high density by increasing packing, preventing the possibility of approaching the fully bonded network state. Along this isochore, the dynamics progressively slows down, first with a super-Arrhenius T dependence (around percolation), then crossing to an Arrhenius dependence at low T. The behavior is similar to that reported for silica and water, where also a cross-over

from super-Arrhenius to Arrhenius behavior has been observed in connection with the establishment of an extensively connected network [32,33]. In the case of silica this cross-over has been interpreted as a manifestation of the mode coupling temperature [34]. In this model, in which bonding is unambiguously defined, it appears that Arrhenius dynamics sets in when most of the particles belong to the spanning cluster. Interestingly, the comparison between the time scales of bond-breaking events and diffusional processes clearly shows that diffusion over long distances (as detected by $F_s(q,t)$) is slaved to the bond lifetime and a truly diffusional process (such that $\tau_s q^2$ is approximately constant) can be observed at very small wavevectors only. The characteristic time scale of the collective dynamics shows oscillations in phase with the structure factor, similarly to what has been found in the case of atomic and molecular glass formers [28–30]. Interestingly, the decay of the density fluctuations does not always require the breaking of bonds. Only at very low T has the gel become so stiff that the decay of the density fluctuations, even on length scales comparable to the particle size, requires the preliminary breakdown of the bond network. Under these conditions, the self- and collective dynamics become slaved to the time scale set by τ_b.

Downloaded By: [Universita di Roma La Sapienza] At: 16:26 1 November 2011

Acknowledgments

It is a great pleasure for us to contribute to the present special issue in honor of Prof. Luciano Reatto, a leading scientist who has significantly contributed to shape, among others, the Italian liquid and soft matter communities. We acknowledge support from ERC-226207-PATCHYCOLLOIDS and ITN-234810-COMPLOIDS as well as from NVIDIA.

References

[1] S.C. Glotzer and M.J. Solomon, Nature Mat. **6**, 557 (2007).
[2] A.B. Pawar and I. Kretzschmar, Macromol. Rapid Comm. **31**, 150 (2010).
[3] E. Bianchi, R. Blaak and C.N. Likos, Phys. Chem. Chem. Phys. **13**, 6397 (2011).
[4] F. Sciortino, E. Bianchi, J.F. Douglas and P. Tartaglia, J. Chem. Phys. **126**, 4903 (2007).
[5] E. Bianchi, J. Largo, P. Tartaglia, E. Zaccarelli and F. Sciortino, Phys. Rev. Lett. **97**, 168301 (2006).
[6] J. Russo, P. Tartaglia and F. Sciortino, J. Chem. Phys. **131**, 014504 (2009).
[7] L. Rovigatti, W. Kob and F. Sciortino, ArXiv e-prints, J. Chem. Phys. **135** (2011).
[8] S. Saw, N.L. Ellegaard, W. Kob and S. Sastry, J. Chem. Phys. **134**, 164506 (2011).
[9] R. Blaak, M.A. Miller and J.P. Hansen, Europhys. Lett. **78**, 26002 (2007).
[10] J. Russo, J.M. Tavares, P.I.C Teixeira, M.M. Telo da Gama and F. Sciortino, Phys. Rev. Lett. **106**, 085703 (2011).
[11] A. Reinhardt, A.J. Williamson, J.P.K Doye, J. Carrete, L.M. Varela and A.A. Louis, J. Chem. Phys. **134**, 104905 (2011).
[12] F. Sciortino, A. Giacometti and G. Pastore, Phys. Rev. Lett. **103**, 237801 (2009).
[13] F. Sciortino, Eur. Phys. J. B **64**, 505 (2007).
[14] E. Zaccarelli, J. Phys.: Condens. Matter **19**, 323101 (2007).
[15] E. Del Gado and W. Kob, Europhys. Lett. **72**, 1032 (2005).
[16] E. Del Gado and W. Kob, Phys. Rev. Lett. **98**, 028303 (2007).
[17] C. De Michele, S. Gabrielli, P. Tartaglia and F. Sciortino, J. Phys. Chem. B **110**, 8064 (2006).
[18] N. Kern and D. Frenkel, J. Chem. Phys. **118**, 9882 (2003).
[19] http://developer.nvidia.com/category/zone/cuda-zone
[20] P.H. Colberg and F. Höfling, Comput. Phys. Commun. **182**, 1120 (2011).
[21] C.R. Trott, L. Winterfeld and P.S. Crozier, ArXiv e-prints (2010).
[22] J.A. Anderson, C.D. Lorenz and A. Travesset, J. Comput. Phys. **227**, 5342 (2008).
[23] P.K. Jha, R. Sknepnek, G.I. Guerrero-García and M. Olvera de la Cruz, J. Chem. Theory Comput. **6**, 3058 (2010).
[24] C.A. Angell, J. Non-Cryst. Solids **131-133**, 13 (1991).
[25] P.H. Poole, S.R. Becker, F. Sciortino and F.W. Starr, ArXiv e-prints (2011) and J. Phys. Chem. B dx.doi.org/10.1021/jp204889m
[26] F.W. Starr and F. Sciortino, J. Phys.: Condens. Matter **18**, L347 (2006).
[27] W. Götze, in *Les Houches Summer Schools of Theoretical Physics Session LI (1989)*, edited by J.P. Hansen, D. Levesque and J.Zinn-Justin (North-Holland, Amsterdam, 1991), pp. 287–503.
[28] F. Sciortino, L. Fabbian, S.H. Chen and P. Tartaglia, Phys. Rev. E **56**, 5397 (1997).
[29] A. Rinaldi, F. Sciortino and P. Tartaglia, Phys. Rev. E **63**, 061210 (2001).
[30] J. Horbach and W. Kob, Phys. Rev. E **64**, 041503 (2001).
[31] B. Ruzicka, E. Zaccarelli, L. Zulian, R. Angelini, M. Sztucki, A. Moussaïd, T. Narayanan and F. Sciortino, Nature Mater. **10**, 56 (2011).
[32] J. Horbach and W. Kob, Phys. Rev. B **60**, 3169 (1999).
[33] F.W. Starr, F. Sciortino and H.E. Stanley, Phys. Rev. E **60**, 6757 (1999).
[34] F. Sciortino and W. Kob, Phys. Rev. Lett. **86**, 648 (2001).